Intramolecular vibrational energy redistribution and the time evolution of molecular fluorescence[a]

Karl F. Freed

The James Franck Institute and the Chemistry Department, The University of Chicago, Chicago, Illinois 60637

Abraham Nitzan[b]

Bell Laboratories, Murray Hill, New Jersey 07974
(Received 16 June 1980; accepted 7 August 1980)

We note the presence of contradictory estimates of intramolecular vibrational relaxation rates in the literature where large molecules in high energy states, corresponding to huge densities of vibrational levels, have been ascribed relaxation rates orders of magnitude smaller than those assigned to smaller molecules with much smaller densities of vibrational levels. This unphysical disparity is explained as arising from vague (or undefined) definitions of intramolecular vibrational relaxation and/or from a consideration of quantities which are not directly measured or measurable. A resolution of a portion of the problem is already well known for electronic relaxation, but the application of those results to a description of the time evolution of the molecular fluorescence, produced during the intramolecular vibrational relaxation of the electronically excited molecules, requires a generalization of the electronic relaxation theory to separate and describe the "unrelaxed" and "relaxed" emission spectra. We provide this general theory of the time variation of the emission spectrum for molecules conforming to both the intermediate and statistical limits of intramolecular vibrational relaxation with emphasis placed upon the distinguishability between these two cases. The intermediate case analysis utilizes egalitarian and random coupling type models with essentially identical conclusions from both. The time evolution and relative yields associated with the emission spectra are described for both continuous and short pulse excitation, and reasons are provided for the absence of observation of time varying emission spectra in the experiments of Smalley and co-workers. Quantum beats are possible in principle in the sparse intermediate case. Their observability depends, however, on the detection method. When the emission spectrum can be resolved, beats are expected only in the frequency integrated intensity.

I. INTRODUCTION

Recent theoretical and experimental results associated with the phenomenon of intramolecular vibrational relaxation (IVR) are characterized by the following two features:

(a) In most cases IVR is not directly observed. Conclusions concerning IVR are reached on the basis of indirect observations (e.g., the agreement of low pressure photodissociation results with the RRKM theory is taken as evidence for rapid IVR).

(b) Different studies yield *estimated* IVR lifetimes spreading over an enormous range. For example, IVR lifetimes for naphthalene T_1 (excess vibrational energy $E_v = 11\,000$ cm^{-1})[1(a)] [see also Ref. 1(b)], for pentacene S_0 ($E_v = 19\,000$ cm^{-1})[2(a)] (see, however, Ref. 3) and for glyoxal S_0 ($E_v = 22\,000$ cm^{-1})[2(b)] were estimated to be long ($\gtrsim 10^{-6}$ sec). On the other hand, the IVR lifetime for SF$_6$ (S_0, $E_v = 1000$–3000 cm^{-1}) was estimated to be of order 1–30 psec[4] (see, however, Ref. 5); the IVR lifetime for dimethyl POPOP (S_1, $E_v = 3000$ cm^{-1}) was estimated to be shorter than 2 psec[6(a)]; that for coumarin 6 (S_0, $E_v = 6000$ cm^{-1}) was estimated as 4 ± 1 psec[6(b)]; the widths of overtone line shapes in benzene[7] and naphthalene[8] (S_0, $E_v = 8000$–$20\,000$ cm^{-1}) correspond to IVR lifetimes of ~ 0.1 psec; and studies

on pressure dependence of rates of thermal reactions involving large molecules indicate vibrational energy redistribution times of the order of ~ 1 psec.[9] It is interesting also to mention that classical trajectory studies on a six oscillator model of benzene using a model potential surface[10] have led to the conclusion that IVR is slow on the picoseconds time scale.

While a wide range of processes and rates are to be expected in a phenomenon associated with coupled anharmonic oscillators, there is an apparent conflict between results that indicate relatively slow IVR rates in molecules excited relatively high in their vibrational manifolds and other results which suggest that IVR is fast even for medium size molecules excited only a few (2–3) thousand wave numbers above the electronic origin. It may be expected that a direct observation of IVR will provide a better picture of the process and resolve the existing difficulties. This is an important point addressed in our paper. The direct observation of intramolecular vibrational relaxation requires, in effect, a dynamical experiment in which a well specified initial vibrational state or superposition thereof is prepared. This initial state decays, and a measurement is made at a subsequent time to demonstrate that the system is then in a state which differs from the originally prepared one. This type of dynamical experiment has been considered for electronic relaxation[11] where, for instance, measurements of triplet–triplet absorption provide a direct confirmation of intersystem crossing from singlets to triplets.

The most widely known studies of "intramolecular

vibrational relaxation" are associated with thermal unimolecular reactions. The RRKM theory is widely accepted as being predicated on the assumption that intramolecular vibrational relaxation is rapid on the time scales of molecular decomposition. The successes of the predictions of RRKM theory have been taken as proof of this vibrational energy randomization. However, the thermal reactions or even the chemical activation experiments are not of the above noted dynamical nature. What is the initially prepared state in these experiments? It most certainly is a statistical superposition of many states by virtue of the random nature of the collisional preparation of the activated species. Perhaps it is this statistical character of the initial state which is responsible for the success of the statistical theories. In fact, the RRKM theory can be formulated in a mechanistic equivalent fashion by assuming that intramolecular vibrational relaxation is slow on the time scales of molecular decomposition.[12] The molecule stays in the initially prepared highly anharmonic vibrational eigenstates. The distribution of molecular lifetimes is *assumed* to be random as in RRKM theory. Note that these two diametrically opposed formulations of the same RRKM theory also take significantly different viewpoints of the meaning of intramolecular vibrational relaxation. The energy randomizing approach views the vibrational states in terms of a zeroth order harmonic description, whereas the nonstatistical theory considers the vibrational eigenstates which diagonalize the full molecular Hamiltonian. The complementarity principle of quantum mechanics tells us that we can formulate a theory in either basis, and the quantum mechanical predictions must be totally independent of the basis set chosen. However, there is a significant difference between these two approaches in their description of the initially prepared excited vibrational states. It is highly improbable that any means of excitation could prepare a molecule with substantial amounts of energy in a pure harmonic mode. Experiments have shown that in the special case of CH vibrations[7,8,13] and also CO vibrations[14] it is possible to prepare a molecule with considerable amounts of energy in this local mode. The subsequent time evolution of this state has to date not yet been followed, and the nature of its intramolecular vibrational relaxation has been inferred from optical linewidths rather than from more definitive time dependent measurements. Similarly, in the case of multiphoton dissociation, the initial state of the system before laser excitation is given by a broad thermal distribution, and the multimode character of the laser excitation also contributes to the inherent statistical nature of the system. We may conclude from this discussion that (a) a correct interpretation of any observed IVR process should take into account the nature of the state prepared, and (b) the interpretation depends on the language (i.e., basis set) used and primary attention should be given to the actual observation rather than to semantic differences between various representations.[15]

Hopkins, Powers, and Smalley[16] have taken an interesting approach towards the problem of the measurement of intramolecular vibrational relaxation processes. They consider alkylated benzenes in a supersonic nozzle where

the cooling of the internal degrees of freedom suppresses the statistical aspects of the initially prepared state that arise from rotational and sequence broadening in higher temperature situations. The experiments find that the absorption spectra due to the $6b$, 12, and $18a$ modes in the first excited singlet S_1 are largely invariant to changes in the type and length of the alkyl chain. However, the fluorescence spectrum arising from the excitation into these three modes varies considerably with the number of vibrational degrees of freedom in the alkyl side group. The emission from the 0^0 level is a typical resonance fluorescence for all of the alkylated benzenes, but the emission from states with excitation in one of these three modes is considerably changed by alkylation. The fluorescence spectrum can display two types of features. One type involves sharp features of a nature analogous to those observed in the 0^0 fluorescence, while the other is a broad red shifted fluorescence spectra that can be assigned to the intramolecularly vibrationally relaxed species. The rate of this intramolecular vibrational relaxation is seemingly enhanced with an increase in the vibrational degree of freedom in the alkyl side group. Such experiments can potentially lead to a direct observation of IVR through the time evolution of the fluorescence spectrum. Using the molecular fluorescence as a probe limits however the range of observable times to that of the fluorescence time scale. In the experiments of the Smalley group[16] no direct observation of the IVR process has been achieved. Estimate of the IVR rates from the relative (relaxed to unrelaxed) yields suggest that for the shorter alkyl chains this IVR should have been observed. Below we consider possible reasons for this lack of observation.

The time evolution of the molecular fluorescence is more directly observed in a recent experiment by Coveleskie, Dolson, and Parmenter.[17] In this experiment, fluorescence quenching by O_2 and NO is used as an internal clock in monitoring IVR in the S_1 manifold of p-difluorobenzene. Without added quencher the fluorescence spectrum obtained following excitation 2190 cm^{-1} above the S_1 origin reveals a sequence of peaks seated on a broad continuum. With consecutively larger quencher pressures the underlying continuum is reduced and analysis of this reduction in conjunction with the quenching efficiency provides an estimate of 10^{-11} sec for the rise time of this continuum. This rise time presumably results from populating states not directly excited via intramolecular vibrational energy redistribution.

Mukamel and Smalley[18] have analyzed the Smalley group experiments both with a simple kinetic model and with a sophisticated stochastic reduction theory which focuses on the measured reduced variables of the system. Both approaches are predicated under the assumption that the vibrational relaxation falls in the statistical limit, i.e., it is an irreversible intramolecular process. Consideration of density of states available in the molecules and the spectral regions studied suggest that the results should more suitably be interpreted in a framework analogous to the intermediate case in the theory of electronic relaxation processes.[19] In this intermediate case the density of final vibrational levels is insufficient to drive

purely irreversible behavior on the time scale of the experiment (which is of order of the fluorescence lifetime).[20,21] The molecule is initially prepared in a superposition of vibrational eigenstates by virtue of the short duration exciting pulse. Under typical experimental conditions where the pulse length is short compared to the lifetime of the excited singlet state, it may be assumed that the molecule is initially prepared in a superposition that corresponds to the zeroth order level assigned in the absorption spectrum. The time evolution of this initial nonstationary state can be described in terms of an initial rapid "intramolecular dephasing process" which appears as if the initial zeroth order state is decaying into the collection of vibrational eigenstates. On these short time scales it is impossible to distinguish between irreversible decay and this dephasing process. The long time decay characteristics of the system are those associated with the vibrational eigenstates of the system. In the literature on electronic relaxation, the intermediate and the statistical cases are clearly distinguished,[20,21] but in most of the work on intramolecular vibrational relaxation this distinction has been blurred, and the two cases are combined into the same category of intramolecular vibrational relaxation. True, both the intermediate and the statistical cases arise from the same physical couplings, but there is a qualitative difference between these limits as well as a wealth of interesting information to be studied by viewing these as separate cases. For instance, using intermediate case theory it is possible to determine the average number of strongly coupled levels and the average coupling strength between the zeroth order level and this set of strongly coupled levels. As we shall see, this distinction between the intermediate and statistical cases also explains the lack of observation of time resolved IVR in the Smalley group experiments with short alkyl chains.

One important difference between the intermediate case theory, as formulated for electronic relaxation,[20] and between the theory needed in the present case is associated with the fact that in the electronic case the dense manifold of levels which is strongly coupled to the initially excited one is nonemitting or is emitting on a time scale much longer than the experimental one [see, however, Ref. 20(a)]. In contrast, the present situation is characterized by a manifold of "final" levels whose emission is monitored during the experiment. Therefore, an appropriate reformulation of the theory used for electronic relaxation is needed, and this is one of the fundamental theoretical problems addressed in this paper. This generalization should include an analysis of the differences predicted by the intermediate and statistical limit theories for the time evolution of the fluorescence spectrum. It is by a consideration of such experiments that we can ask whether measurements can be made to distinguish between intermediate case and statistical limit behavior and thus to determine the threshold for irreversible vibrational relaxation.

In Sec. II we introduce the molecular model and the notation in terms of which the IVR problem is discussed. In Sec. III we briefly discuss long time (line shape) experiments. Short time (time resolved) experiments are discussed in Sec. IV for both the intermediate and the

statistical cases. In Sec. V we address a particular aspect of short time experiments: the possibility of observing temporal beats in the evolution of the fluorescence. Our results are summarized in Sec. VI.

II. THE MOLECULAR MODEL

It is convenient to discuss the molecular model in terms of the ideal jet experiment in which the molecule is initially in the ground vibrational rotational level of the ground electronic state. This level is denoted $|g, 0, 0\rangle$. For the sake of definiteness we consider excitation into the set of molecular vibronic levels associated with the first excited molecular singlet. Electronic radiationless relaxation is disregarded for now, but its role is discussed later. The usual spectroscopist's approach is to assign the spectrum in terms of a basis set of zero order levels based on the populations of a set of zero order modes (normal modes, symmetrized local bond modes, etc.). The latter may be divided into two groups which we denote by a (active) and b (bath). The a modes are those whose corresponding potential surfaces in the ground (g) and excited (e) electronic states differ appreciably from each other. The other b modes do not change or change very little during the electronic transition. The a modes thus correspond to the different progressions in the molecular absorption spectrum. The zero order molecular vibronic levels are denoted $|g, n_{ga}, n_{gb}\rangle$ and $|e, n_{ea}, n_{eb}\rangle$, where $n_{ia,ib}$ ($i = g, e$) denote the populations of the a and b modes in the g and e electronic states. It should be noted that n_{ia} and n_{ib} are shorthand notations for $\{n_{ia}^{\alpha}\}$ and $\{n_{ib}^{\beta}\}$, where α and β denote the different modes of the groups a and b, respectively. Sometimes, when no confusion may arise we drop the subscripts g and e on the mode populations (i.e., $|e, n_a, n_b\rangle \equiv |e, n_{ea}, n_{eb}\rangle$). Also, in some cases we replace the pair n_a, n_b by the single letter n (i.e., $|e, n_a, n_b\rangle \equiv |e, n\rangle$).

In monitoring the molecular fluorescence we in fact follow the populations of the a modes. The appropriate molecular model (Fig. 1) is composed of manifolds of b states seated on the different states of the a mode. All these states are eigenstates of the zero order molecular Hamiltonian H_0^M. The total Hamiltonian is

$$H = H_0 + \mu + W ,\tag{II.1}$$

$$H_0 = H_0^M + H_0^R ,\tag{II.2}$$

where H_0^R is the Hamiltonian of the free radiation field, μ is the molecule–radiation field interaction which couples the e and g states, and W is the intramolecular vibrational interaction which couples the different a and b modes. IVR is viewed as transitions between the manifolds shown in Fig. 1, induced by the coupling W.

For the alkyl substituted benzene molecules studied by Smalley et al.[16] we can specify the model somewhat further: In these systems it is observed that some modes (in particular those assigned as the 6b, 12, and 18a ring modes) are not appreciably affected by changing the alkyl side chains. In their studies on IVR, Smalley et al. have chosen to follow excitation and fluorescence which correspond to transitions associated with these modes. These modes therefore constitute the a group
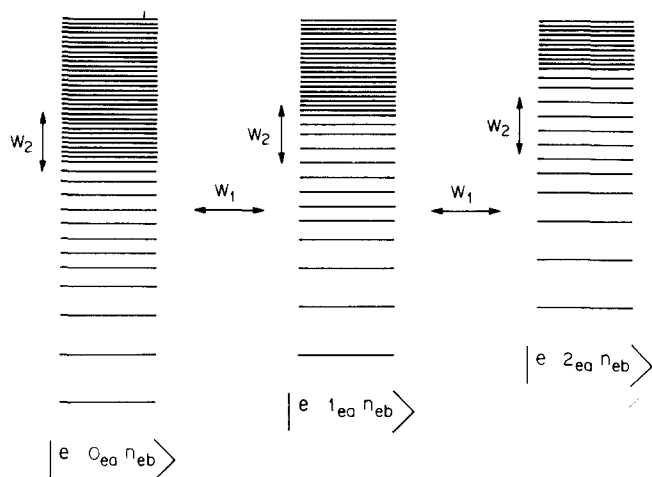
FIG. 1. The molecular model used in the discussion of intra-molecular vibrational relaxation (IVR) in an excited electronic state ($|e\rangle$). Each manifold corresponds to a particular state of the optically active (a) modes and is composed of levels associated with different states of all other (bath b) modes. W_1 denotes an intramolecular coupling between the a modes and the b modes (which leads to processes which change the a modes populations). W_2 denotes the coupling between the b modes.

in our model. The fact that they are not sensitive to changes in the alkyl side chains imples that the presence of these side chains does not enormously affect the magnitude of the coupling W_1 (Fig. 1) between the a and the b modes. The main effect of adding the side chains is therefore to change the density of bath states and possibly to change "intrabath" coupling W_2. The dynamics, in contrast, can be substantially altered by smaller changes in W_1 than those affecting the spectrum.

Fluorescence spectra

A narrow pulse excitation of the molecule, originally in the state $|g,\ 0,\ 0\rangle$, transports the molecule to the state $|e,\ \{n_{ea}^{\alpha}\},\ \{0_{eb}^{\beta}\}\rangle$. The fluorescence corresponding to a transition from this state to the ground level $|g,\ \{n_{ga}^{\alpha}\},\ \{0_{gb}^{\beta}\}\rangle$ is characterized by the frequency

$$\omega = E_{eg}/\hbar + \sum_{\alpha}(\omega_{e\alpha}\, n_{ea}^{\alpha} - \omega_{g\alpha}\, n_{ga}^{\alpha})\ , \tag{II.3}$$

where $E_{eg}/\hbar$ is the transition frequency of the origin. The *corresponding* "relaxed" transition from the state $|e,\ \{n_{ea}^{\alpha\prime}\},\ \{n_{eb}^{\beta\prime}\}\rangle$, which is quasidegenerate with the originally excited state (i.e., $\sum_{\alpha}\omega_{e\alpha}\, n_{ea}^{\alpha}\cong\sum_{\alpha}\omega_{e\alpha}\, n_{ea}^{\alpha\prime}$ $+\sum_{\beta}\omega_{e\beta}\, n_{eb}^{\beta\prime})$ is characterized by the frequency

$$\omega' = E_{eg}/\hbar + \sum_{\alpha}(\omega_{e\alpha}\, n_{ea}^{\alpha\prime} - \omega_{g\alpha}\, n_{ga}^{\alpha\prime}) + \sum_{\beta}(\omega_{e\beta}\, n_{eb}^{\beta\prime} - \omega_{g\beta}\, n_{gb}^{\beta\prime}) \tag{II.4}$$

where $n_{ea}^{\alpha\prime} - n_{ga}^{\alpha\prime} = n_{ea}^{\alpha} - n_{ga}^{\alpha}$ and $n_{eb}^{\beta\prime} = n_{gb}^{\beta\prime}$. This frequency is shifted relative to the original frequency by the amount

$$\omega' - \omega = \sum_{\alpha}(\omega_{g\alpha} - \omega_{e\alpha})(n_{ea}^{\alpha} - n_{ea}^{\alpha\prime}) - \sum_{\beta}(\omega_{g\beta} - \omega_{e\beta})\, n_{eb}^{\beta\prime}\ . \tag{II.5}$$

Normally, $\omega_{g\nu} > \omega_{e\nu}$ ($\nu = \alpha,\ \beta$) and also $n_{ea}^{\alpha} > n_{ea}^{\alpha\prime}$. Therefore, the two terms on the right hand side of Eq. (II.5) are positive. Depending on the relative absolute magnitudes of these two terms, the relaxed emission is shifted to the red or to the blue relative to the "un-relaxed" one. Because of the large number of states $|e,\ \{n_{ea}^{\alpha\prime}\},\ \{n_{eb}^{\beta\prime}\}\rangle$ contributing to the relaxed emission, it appears broader than the unrelaxed emission. This broadening reflects the collection of different emission lines associated with different populations of bath modes according to Eq. (II.5). We note that in the experiments of Smalley et al.[16] the relaxed emission appears on the blue side of the unrelaxed line, reflecting the fact that the frequency changes in the b modes are smaller than those in the a modes. Another interesting feature is the fact that the relaxed emission becomes less diffuse in going to substituted benzenes with larger alkyl chains.[16] This phenomenon reflects the fact that for longer side chains most of the b modes are associated with chain motions that are not affected by the electronic transition. For such modes $\omega_{g\beta} = \omega_{e\beta}$ and they do not contribute to the shift (II.5),[16] but they still can affect the intramolecular vibrational dynamics.

"Exact" molecular states

As in many treatments of intramolecular relaxation we find it sometimes advantageous to analyze the system not in terms of the zero order states (eigenstates of H_0 $= H_0^M + H_0^R$) but rather using the exact molecular basis set (eigenstates of $H_0^M + W + H_0^R$). These states can be written as linear combinations of the zero order states

$$\psi_{ej} = \sum_{n_a, n_b} C_{n_a, n_b}|e,\ n_a,\ n_b\rangle \equiv |e, j\rangle\ . \tag{II.6}$$

In particular, a narrow pulse which promotes a transition from $|g,\ 0,\ 0\rangle$ to a particular zero order level $|e,\ n_a,\ 0\rangle$ involves in the exact molecular state picture those exact $|e, j\rangle$ which contain contribution from $|e,\ n_a,\ 0\rangle$:

$$|e, j\rangle = A_{j;n_a,0}|e,\ n_a,\ 0\rangle + \sum_{n_a', n_b'} B_{j;n_a',n_b'}|e,\ n_a',\ n_b'\rangle\ . \tag{II.7}$$

Assuming that the intramolecular coupling W is much smaller than the energy spacing between the primary zero order states $|e,\ n_a,\ 0\rangle$ (for different $n_a \equiv \{n_a^{\alpha}\}$) leads to the following picture: Each exact $|e, j\rangle$ state corresponds to a single zero order primary $|e,\ n_a,\ 0\rangle$ state and a group of quasidegenerate $|e,\ n_a',\ n_b'\rangle$ states with $n_a' < n_a$.[19] The number of zero order states contributing to the right hand side of Eq. (II.7) is of order $(|W|\rho)^2$, where ρ is the density of levels in the $\{|e,\ n_a',\ n_b'\rangle\}$ manifold.

Fluorescence lifetimes

In the Condon approximation the total radiative lifetimes of the different rovibronic levels $|e,\ n_a,\ n_b\rangle$ are the same for all levels. Therefore, the same is also true for the levels $|e, j\rangle$ which diagonalize the molecular Hamiltonian. The total width of a zero order molecular level $|e, n\rangle\ [n \equiv (n_a,\ n_b)]$ is
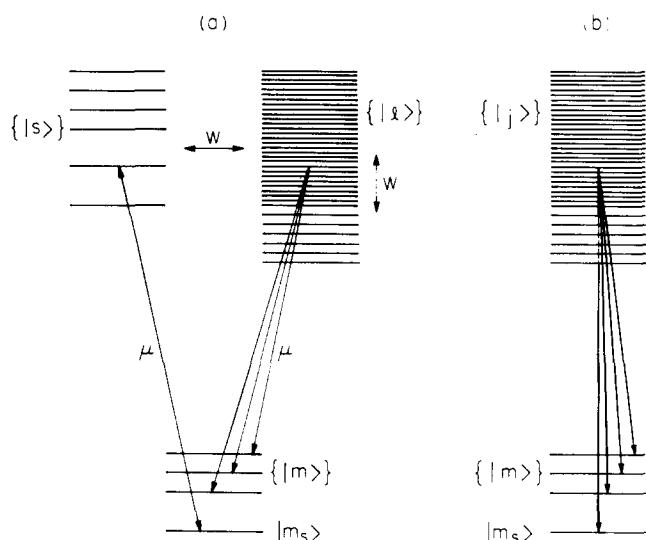
FIG. 2. A simplified molecular model. (a) $|s\rangle$ are zero order levels belonging to the excited electronic state which are directly accessible from the initial ground state level $|m_s\rangle$. The intramolecular zero order bath levels are $\{|l\rangle\}$. (b) The corresponding exact molecular state picture.

$$\gamma_n = \gamma^R + \gamma_n^{NR} . \qquad (\text{II. 8})$$

γ^R is the radiative width and γ_n^{NR} is the nonradiative width associated with radiationless electronic transitions.[23]

Simplified model

Keeping in mind that the molecular model is represented in all relevant details in Fig. 1, it is sometimes convenient to discuss the IVR problem using a more simplified model as follows: If the molecule is initially cold (i.e., in the state $|g, 0, 0\rangle$) an incident beam or pulse which is narrow enough in energy may effectively couple the initial state to a single $|e, n_a, 0\rangle$ level. This is true provided that the spacing between $|e, n_a, 0\rangle$ states is larger than the bandwidth of the incident radiation. Under these conditions the excited zero order states which participate in the absorption–emission process are the state $|e, n_a, 0\rangle$ and the group of states $|e, n_a', n_b'\rangle$ which are quasidegenerate with it (to within an energy range of order $|W|$). The latter are radiatively coupled to ground levels other than $|g, n_a'', 0\rangle$ (to which $|e, n_a, 0\rangle$ is coupled), and this gives rise to the relaxed fluorescence. Disregard all other molecular states and denote

$$|e, n_a, 0\rangle \equiv |s\rangle \quad \{|e, n_a', n_b'\rangle\} \equiv \{|l\rangle\} .$$

Ground state levels to which $|s\rangle$ and $\{|l\rangle\}$ are coupled radiatively are denoted $\{|m\rangle\}$. We sometime use $|m_s\rangle$ to denote a level (like $|g, 0, 0\rangle$) which couples to $|s\rangle$ but not to the states $|l\rangle$. The model is shown in Fig. 2(a). In the corresponding exact molecular states representation [Fig. 2(b)] the group of levels $|s\rangle$, $\{|l\rangle\}$ is replaced by the group $\{|j\rangle\}$ which are obtained as linear combinations of $|s\rangle$ and $\{|l\rangle\}$ states which diagonalize the Hamiltonian $H_0^M + W$.

The most significant difference between the model discussed here and similar models used before for the electronic radiationless transitions problem lies in the fact that the underlying continua (Fig. 1), which provide the sink for the decay of the initially prepared level, are optically active: the emission from these states constitutes the relaxed part of the fluorescence as discussed above. In what follows we explore the implication of this consecutive emission process on the line shape and time evolution of molecular fluorescence spectra.

III. LONG TIME EXPERIMENTS

In the intermediate level structure case the decay width γ_j [Eq. (II. 9)] of the individual exact molecular levels are smaller than their averaged spacing

$$\gamma_j < \hbar \rho^{-1} , \qquad (\text{III. 1})$$

with ρ being the density of states. This implies that in a continuous excitation experiment or using a pulse long enough to resolve the individual levels, the resulting fluorescence is that characterizing an individual level $|e, j\rangle$ [Eq. (II. 7)]. This immediately leads to the following conclusions:

(a) In a long time pulse experiment the fluorescence decays exponentially with lifetime $\tau_j = \hbar / \gamma_j$.

(b) The fluorescence yield in this case is γ^R / γ_j.

(c) The lifetime τ_j and yield γ^R / γ_j vary from level to level, reflecting changes in γ_j due to variations in the rates of electronic radiationless transitions.

(d) The relative intensities of different absorption or fluorescence excitation lines (corresponding to different $|e, j\rangle$ levels) are given by $|A_{j;n_a,0}|^2$ [c.f. Eq. (II. 7)].

(e) The ratio between the integrated unrelaxed and relaxed emissions is given $|A_{j;n_a,0}|^2 (1 - |A_{j;n_a,0}|^2)^{-1}$.

(f) The fluorescence spectrum does not evolve in time.

These conclusions correspond to the ideal case where the molecule is initially in the ground state $|g, 0, 0\rangle$. Unfortunately, even in the current supersonic jet experiments[16] the rotational temperature in the jet is ~ 2 °K so that for the molecules studied the average rotational quantum number is ~ 10. Hence, the fluorescence excitation spectrum involves a superposition of contributions from many different rotational levels, and this is expected to wash out the above described structure. By further rotational cooling and the use of monochromatic lasers (orthogonal to the molecular beam direction to reduce Doppler broadening and the concomitant overlapping of lines), it should be possible to observe the structure in the relaxed and unrelaxed excitation spectrum associated with the individual $|e, j\rangle$ levels. Note that the IVR does not lead to broadening of individually resolved molecular transitions in the intermediate case, whereas there is broadening the extreme statistical limit. As the density of states increases, the energy spacing ρ^{-1} becomes smaller than the widths $\hbar \gamma_j$ so it becomes impossible to selectively excite a single molecular eigenstate even with an ideally monochromatic radiation.

In the statistical limit the manifolds $|e, n_a', n_b'\rangle$ $(n_a' < n_a)$[22] become dissipative continua for intramolecular decay of the initially excited level $|e, n_a, 0\rangle$. The decay rate is then given by the golden rule formula

$$\Gamma_n = 2\pi \sum_{n_a' < n_a} \left\{ \sum_{n_b'} |\langle e, n | W | e, n' \rangle|^2 \right.$$

$$\left. \times \delta \left[\sum_\alpha \omega_{e\alpha} n_a^\alpha - \left(\sum_\alpha \omega_{e\alpha} n_a^{\alpha'} - \sum_\beta \omega_{e\beta} n_b^{\beta'} \right) \right] \right\},$$

(III.2)

where n and n' are shorthand notations for $(n_a, 0)$ and (n_a', n_b'), respectively. The absorption line shape to the resonance centered around the zero order state $|e, n, 0\rangle$ becomes in the extreme statistical limit approximately a Lorentzian with a width $\Gamma_n + \gamma_n$ consisting of contributions corresponding to vibrational, radiationless electronic, and radiative relaxation. Simple kinetic calculation then leads to the yields for the direct (unrelaxed) emission Y_{dir} and for the relaxed emission Y_{rel}:

$$Y_{dir} = \frac{\gamma^R}{\gamma^R + \gamma^{NR} + \Gamma},$$

(III.3)

$$Y_{rel} = \frac{\gamma^R \Gamma}{(\gamma^R + \gamma^{NR})(\gamma^R + \gamma^{NR} + \Gamma)}.$$

(III.4)

The total emission yield is

$$Y_{dir} + Y_{rel} = \frac{\gamma^R}{\gamma^R + \gamma^{NR}}$$

(III.5)

and the relative yield of the relaxed vs the direct emission is

$$\frac{Y_{rel}}{Y_{dir}} = \frac{\Gamma}{\gamma^R + \gamma^{NR}}.$$

(III.6)

These yields are independent of the excitation frequency within the absorption profile of the $|e, n\rangle$ resonance. These results are obtained under the simplifying assumption that γ^{NR} (electronic radiationless relaxation rate) is the same for all levels. The kinetic approach may be justified[24,25] for the present model for which the random nature of the coupling matrix elements insures the absence of interference effects.

Equation (III.6) implies that the relative yield Y_{rel}/Y_{dir} of the relaxed and direct fluorescence may be made smaller by adding an efficient fluorescence quencher, thereby increasing γ^{NR}. This is the basis for the experiment of Parmenter et al.,[17] who use O_2 and NO as quenchers of the p-difluorobenzene fluorescence. The requirement for a quencher of high efficiency is necessary to insure that γ^{NR} is affected without Γ (IVR rate) increasing at the same time due to quasielastic collisions with the quencher molecules. It is interesting to point out the similarity between the present situation and the circumstances governing resonance Raman scattering from thermally relaxing systems.[24,26] In that case efficient quenchers may be used to change the relative yields of the Raman and the fluorescence components of the scattered light.

IV. SHORT TIME EXPERIMENTS

We now consider the case where the excitation pulse is short enough in time and broad enough in energy so
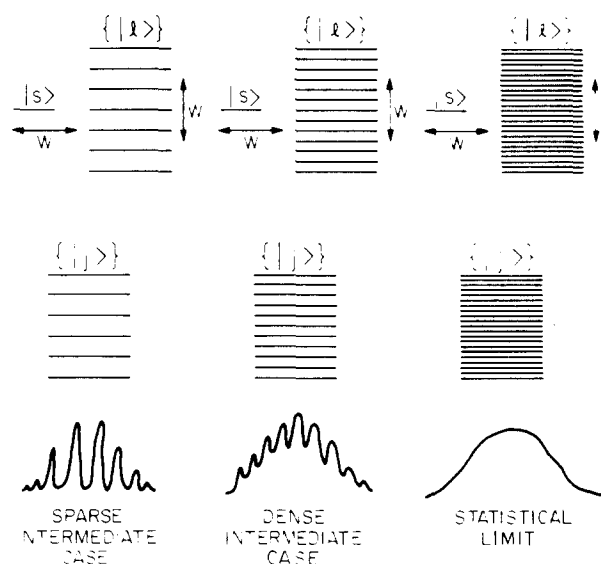

FIG. 3. Zero order level structure (upper), exact molecular level structure (middle), and the corresponding absorption spectrum associated with the sparse intermediate case (left), the dense intermediate case (middle), and the statistical limit (right).

that a zero order nonstationary state $|e, n_a, 0\rangle$ is initially prepared. In terms of the exact molecular states $|e, j\rangle$ the initial state is [cf Eq. (II.7)]

$$\Psi(0) = |e, n_a, 0\rangle = \sum_j A^*_{j;n_a,0}|e, j\rangle.$$

To achieve this initial excitation the pulse time has to be much shorter than the inverse energy span of the states $|e, j\rangle$ with $A_{j;n_a,0} \neq 0$. The pulse bandwidth has to be smaller than the energy spacing between $|e, n_a, 0\rangle$ levels. Assuming that these conditions hold, we can analyze the molecular relaxation and the time evolution of the molecular fluorescence using the simplified model defined in Sec. II and represented by Fig. 2. In terms of this model the zero order level structure, the corresponding exact states manifold, and a characteristic absorption spectrum corresponding to the sparse intermediate (level spacings larger than level widths), the dense intermediate (level spacings of the order of level widths) and the statistical (level spacings much smaller then level widths) cases are shown in Fig. 3. Note that by "level widths" we mean the sum of the radiative and the electronic radiationless decay widths, but not widths associated with IVR.

The significance of the emission spectra displayed in Fig. 3 needs further clarification. For this we focus on two emission lines which correspond to two different *final* (ground state) levels $|m_s\rangle$ and $|m_r\rangle$. Suppose that in the zero order representation $|m_s\rangle$ is exclusively coupled (via the molecule–radiation field interaction μ) to $|s\rangle$ while $|m_r\rangle$ is coupled to another zero order level $|r\rangle$ which belongs to the $\{|l\rangle\}$ manifold.[27] Figure 4 shows this situation in the dense intermediate case together with a schematic description of the emission line shape for the transitions which end in the $|m_s\rangle$ and $|m_r\rangle$ levels. We note that by definition the $|s\rangle \rightarrow |m_s\rangle$ emission constitutes a "line" in the direct (unrelaxed) fluorescence
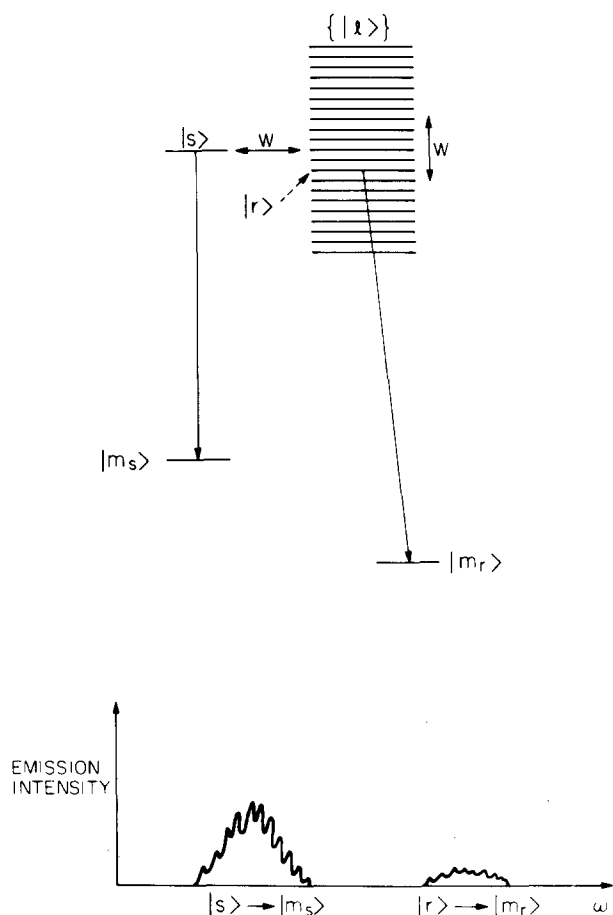
FIG. 4. Direct (unrelaxed, $|s\rangle \rightarrow |m_s\rangle$) and indirect (relaxed, $|r\rangle \rightarrow |m_r\rangle$) emissions in the simplified molecular model. Note that the $|r\rangle \rightarrow |m_r\rangle$ emission is only one component contributing to the total relaxed fluorescence.

spectrum while the $|r\rangle \rightarrow |m_s\rangle$ emission constitutes one (of many overlapping) contribution to the relaxed emission. $|s\rangle$ and $|r\rangle$ are however linear combinations of the exact energy states $|j\rangle$, i.e., $|s\rangle = \sum_j a_{sj}|j\rangle$ and $|r\rangle = \sum_j a_{rj}|j\rangle$. Therefore, in the intermediate case each of these lines can in principle be resolved to separate lines corresponding to the different $|j\rangle$ levels as shown in Figs. 3 and 4.

In Appendix A we prove the following theorem: At any time following the initial preparation of the excited molecule, the integrated intensity of the emission associated with the transition into the ground level $|m_b\rangle$ is proportional to the population in level $|p\rangle$, i.e., $|\langle p|\Psi(t)\rangle|^2$, where $\Psi(t)$ is the molecular state at time t, and $|p\rangle$ is the excited zero order level which carries all the oscillator strength for transitions from $|m_b\rangle$ in the spectral region of interest.[21(b)] Note that $|p\rangle$ can be the initially excited level $|s\rangle$ or any other zero order level belonging to the manifold $\{|l\rangle\}$.

The validity of discussing the time evolution of molecular emission spectra in terms of populations of zero order molecular levels has been taken for granted in many past works.[28] The theorem proven in Appendix A may however have profound consequences as discussed in the next section.

In the rest of this section we assume (as is indeed usually the case) that the condition under which the populations of the zero order levels determine the instantaneous emission spectra is satisfied. The intensity of the direct (unrelaxed) emission at time t is proportional to the population $P_s(t) = |\langle s|\exp(-iHt)|s\rangle|^2$ and the spectrally integrated intensity of the relaxed emission at time t is proportional to

$$P_L(t) \equiv \sum_l P_l(t) = \sum_l |\langle l|\exp(iHt)|s\rangle|^2 .$$

The intermediate case

The evolution within the $|s\rangle - \{|l\rangle\}$ manifold in the model described in Fig. 4 has been intensively studied in connection with the theory of intramolecular electronic relaxation. In the intermediate case the population $P_s(t)$ evolves differently at short and long times. Immediately following the excitation $[\Psi(t=0) = |s\rangle]$ and during a time short compared to the inverse level spacing in the $\{|l\rangle\}$ manifold, the $\{|l\rangle\}$ manifold behaves as a continuum and the evolution of $P_s(t)$ proceeds as in the statistical limit (see below). The direct emission decays with the total rate $\gamma_s + \Gamma$, where γ_s is the sum of the radiative and electronic radiationless widths of the levels $|s\rangle$ while Γ is given by

$$\Gamma = 2\pi \sum |W_{sl}|^2 \frac{1}{\pi} \frac{(\tfrac{1}{2})(\gamma_l + \epsilon_0)}{(E_s - E_l)^2 + (\tfrac{1}{4})(\gamma_l + \epsilon_0)^2}$$

$$\simeq 2\pi \overline{|W_{sl}|^2 \rho_l} , \tag{IV.1}$$

where γ_l is the sum of the radiative and electronic radiationless widths of the level $|l\rangle$, ρ_l is the density of levels in the $\{|l\rangle\}$ manifold and ϵ_0 is the uncertainty width (of order τ_0^{-1}) associated with the short observation time τ_0.[29]

At long time (t greater than the inverse level spacing ρ_l), "dephasing" between the different levels due to their slightly different energies has taken place. The situation is best described in terms of the exact molecular levels $|j\rangle$. The initial state is

$$\Psi(t=0) = |s\rangle = \sum_j a_{sj}|j\rangle , \tag{IV.2}$$

and at time t it evolves to

$$\Psi(t) = \sum_j a_{sj}\exp(-iE_j t - \gamma_j t)|j\rangle . \tag{IV.3}$$

Equation (IV.3) is based on the assumption that the damping matrix associated with the exact molecular states $|j\rangle$ is diagonal. This may be justified for the radiationless part of γ_j invoking the random-like nature of intramolecular coupling between vibrational levels. It is true also for the radiative part of γ_j because of the fact that the total radiative lifetime is the same for all rovibronic levels belonging to a given electronic state. Equation (IV.3) leads to

$$P_s(t) = |\langle s|\Psi(t)\rangle|^2 = \sum_j |a_{sj}|^4 \exp(-\gamma_j t)$$

$$+ 2 \sum_{j \neq j'} |a_{sj}|^2 |a_{sj'}|^2 \exp[-\tfrac{1}{2}(\gamma_j + \gamma_{j'})t]\cos(\omega_{jj'}t) ,$$

$$\tag{IV.4}$$

where $\hbar\omega_{jj'} = E_j - E_{j'}$. The second term in the rhs of Eq. (IV.4) describes quantum beats in the fluorescence. However, when more than a few (~ 10) levels contribute, the sum of oscillating terms averages for $t > \rho_j$ to a vanishingly small contribution. This subject is further discussed in the next section. When these oscillations may be disregarded we obtain (for long enough time)

$$P_s(t) = \sum_j |a_{sj}|^4 \exp(-\gamma_j t) . \qquad \text{(IV.5)}$$

If there are $\sim N > 2$ strongly coupled s and l levels participating in this process, we may invoke the simplest statistical model of egalitarian mixing so that

$$|a_{sj}|^2 = N^{-1} . \qquad \text{(IV.6)}$$

We then have

$$P_s(t) = \begin{cases} \exp[-(\gamma_s + \Gamma)t] & \text{(short time)} , \\ \dfrac{1}{N} \exp(-\gamma_j t) & \text{(long time)} . \end{cases} \qquad \text{(IV.7)}$$

The number N of effectively coupled levels may be estimated from

$$N \simeq \Gamma\rho = 2\pi |W|^2 \rho^2 . \qquad \text{(IV.8)}$$

The only difference between the present situation and between that encountered in the theory of electronic relaxation lies in the fact that in most electronic relaxation problems the real life counterpart of the manifold $\{|l\rangle\}$ does not carry significant oscillator strength for radiative emission. The observed radiative lifetime (the radiative part in γ_j) is then of order γ_s^R/N. This has been discussed in terms of the "anomalously" long radiative lifetimes associated with intermediate level structure cases. In the present problem γ_s^R, γ_l^R, and γ_j^R are all equal.

The level width γ_s ($= \gamma_s^R + \gamma_s^{NR}$) and γ_l ($= \gamma_l^R + \gamma_l^{NR}$) are of the same order of magnitude. If we make the simplifying assumption that they are the same (which is rigorously true if variations in γ^{NR} may be neglected), we can obtain also the time evolution of the integrated relaxed fluorescence. The individual $P_l(t)$ are fluctuations within the egalitarian model, having zero average. Their sum, however, is readily evaluated by using the sum rule. For this we use the sum rule

$$P_s(t) + \sum_l P_l(t) = \exp(-\gamma t) , \qquad \text{(IV.9)}$$

where $\gamma = \gamma_s = \gamma_l$, to obtain

$$\sum_l P_l(t) = \begin{cases} \exp(-\gamma t)[1 - \exp(-\Gamma t)] & \text{(short time)} , \\ \dfrac{N-1}{N} \exp(-\gamma t) & \text{(long time)} . \end{cases} \qquad \text{(IV.10)}$$

Equations (IV.7) and (IV.10) lead to the following important conclusion: When quantum beats in the fluorescence are absent, the time evolution of the molecular fluorescence spectrum (i.e., transfer of intensity from direct to relaxed emission bands) takes place only during the initial short dephasing period. This may be also concluded using the exact molecular states representa-

tion: Following the initial dephasing, each level $|j\rangle$ evolves in time essentially independently of other levels and contributes to the emission spectrum direct and relaxed components as discussed in Sec. III. These components decay with the lifetime γ_j and any evolution in the structure of the emission spectrum in the postdephasing period is due to the accidental differences between the different lifetimes γ_j^{-1} of the different j levels.

The statistical limit

As is seen from Eq. (IV.7), as the number N of effectively coupled levels within the $|s\rangle-\{|l\rangle\}$ manifold becomes very large, the long time component in the evolution of $P_s(t)$ becomes negligibly small; P_s decays exponentially practically to zero with the rate $\gamma_s + \Gamma$. In most cases of electronic radiationless relaxation, fluorescence is observed to decay on this time scale. In the present case Eq. (IV.10) indicates that the total population of the $\{|l\rangle\}$ states (which determine the intensity of the relaxed fluorescence) decay on the long time scale with rate $\gamma = \langle\gamma\rangle$ following an initial rapid rise. The situation is similar to that discussed by Nitzan, Jortner and Rentzepis[20(a)] in connection with consecutive electronic relaxation. It is important to note that as long as quantum beats are not observed and as long as no attempt is made to resolve the intermediate level structure in the emission, *the statistical limit and the intermediate case differ only by the magnitude of the number N which enters into Eqs. (IV.7) and (IV.10) as well as (IV.15) and (IV.16) below.*

An interesting question that has not been addressed before concerns the population of different levels $|l\rangle$ in the $\{|l\rangle\}$ manifold during the vibrational relaxation. Let us consider again the model shown in Fig. 4, and focus our attention on the statistical limit (or the short time evolution in intermediate cases). Usually, the time evolution within the $|s\rangle-\{|l\rangle\}$ manifold is determined by disregarding the anharmonic coupling W between the $|l\rangle$ levels (denoted by W_2 in Fig. 1). The usual argument given is that as long as we are interested only in $P_s(t)$ we can perform a partial diagonalization of the Hamiltonian matrix and obtain a set of $\{|l\rangle\}$ states which are not mutually coupled. The results for the populations $P_s(t)$ and $P_l(t)$ for this case are well known[30]:

$$P_s(t) = \exp[-(\gamma + \Gamma)t] , \qquad \text{(IV.11a)}$$

$$P_l(t) = \frac{|W_{ls}|^2 \exp(-\gamma t)}{E_{ls}^2 + (\frac{1}{2}\Gamma)^2}[1 + \exp(-\Gamma t)$$
$$- 2\exp(-\tfrac{1}{2}\Gamma t)\cos(E_{ls} t)] , \qquad \text{(IV.11b)}$$

where $E_{ls} = E_l - E_s$ and $\Gamma = 2\pi \overline{W_{sl}^2}\rho_l$ and where γ is the sum of radiative and electronic radiationless widths. In the present case we are interested not only in $P_s(t)$ but also in $P_l(t)$. It is $\sum_l P_l(t)$ which determines the integrated relaxed fluorescence is given by Eq. (IV.10). Individual populations $P_l(t)$ may be useful for sorting out different contributions to the relaxed spectrum. For this purpose we would like to keep the original character and symmetry of the $|l\rangle$ states, and in particular the selection rules associated with their symmetry. We therefore

need a solution to the problem where the coupling between the $|l\rangle$ states is not disregarded.

Such a solution may be obtained in the statistical limit within the framework of the random coupling model.[31–33] In this model we regard the coupling matrix elements between any two states in the $|s\rangle-\{|l\rangle\}$ manifold as essentially a random function of the state index. This picture is justified for matrix elements involving excited vibrational wave functions because of the highly oscillatory nature of these functions. The validity of these methods for a *single* matrix has been demonstrated numerically.[33] We are now interested in $P_s(t)$ and $P_r(t)$, given that $P_s(t=0)=1$, where the levels $|r\rangle$ and $|s\rangle$ are particular members of a dense set of mutually coupled states. The level $|s\rangle$ is unique only because it is the only one accessible from the ground state and therefore may be initially prepared. A similar model has been recently considered by Beck and Mukamel.[34] An outline of the mathematical approach to this problem is given in Appendix B. The results are

$$P_s(t) = \exp[-(\gamma+\Gamma)t] \qquad \text{(IV.12a)}$$

and

$$P_r(t) = \frac{2\langle W^2\rangle \exp(-\gamma t)}{E_{rs}^2 + \Gamma^2}$$
$$\times \{1 - \exp(-\Gamma t)\cos(E_{rs}t) - \Gamma/E_{rs}\exp[-\Gamma t \sin(E_{rs}t)]\} \qquad \text{(IV.12b)}$$

We see that as expected the time evolution of the initially populated state is the same for this model as for the simplified model which leads to Eq. (IV.11). The time dependence of $P_r(t)$ $(r \neq s)$ is different, but the qualitative behavior is similar. The most significant difference between Eqs. (IV.11b) and (IV.12b) lies in the fact that Eqs. (IV.12b) predicts that the population spread over zero order levels in a (zero order) energy range twice as large as that obtained in Eq. (IV.11b). This result is understandable in view of the fact that in the model which leads to Eq. (IV.12b) each level has an anharmonic width Γ while in the model without coupling between $\{|l\rangle\}$ levels, only the initially excited level is assigned such a width.

Transition from the intermediate case to the statistical limit

Consider now the alkyl substituted benzene molecules studied by Smalley and co-workers.[16] As the alkyl chain becomes longer, the molecule goes from an intermediate case to the statistical limit (see Fig. 3). Because the coupling interaction is channeled through the motion of the substituted benzene carbon and its neighboring alkyl carbon atom, it is anticipated that the total coupling strength summed over all of the bath states is independent of the alkyl chain length to a first approximation. In the intermediate case this coupling is partitioned between N strongly coupled levels, so

$$\langle s|W|l\rangle \simeq \langle s|W|l_0\rangle N^{-1/2} , \qquad \text{(IV.13a)}$$

where $|l_0\rangle$ denotes the relative vibration of the bonded benzene and alkyl carbon atoms, and the $N^{-1/2}$ factor appears because in the egalitarian model this coupling bond vibration is taken to be equally distributed among the N coupled bath levels. Since the density of coupled levels is proportional to N as

$$\rho \simeq \rho_0 N , \qquad \text{(IV.13b)}$$

the overall IVR rate

$$\Gamma = \frac{2\pi}{\hbar} \sum_l |W_{sl}|^2 \rho \simeq \frac{2\pi}{\hbar} |W_{sl_0}|^2 \rho_0 \qquad \text{(IV.14)}$$

is independent of N to a first approximation as described in Fig. 3. As discussed above, the structure of the molecular fluorescence spectrum evolves in time only during the time scale Γ^{-1}. We therefore expect that *so long as intramolecular vibrational relaxation is identified with changes in the fluorescence structure, no great difference in the relaxation rate is expected to be observed for the different alkylbenzenes.* This is indeed the observed behavior. As the density of levels is increased, the relative yields of the direct and relaxed emissions is changing. This feature is explained for $N>2$ by using the egalitarian mixing intermediate case model for the $|a|^2$ and by replacing the $\sum_{j\neq j} \cdot \cos\omega_{jj} \cdot t$ term in Eq. (IV.4) by the exponentially dephasing decay $\exp(-\Gamma t)$ to calculate the unrelaxed (direct) yield from Eq. (IV.4) as

$$Y_{\text{dir}} \simeq \frac{\gamma^R}{N\gamma} + \frac{\gamma^R}{\gamma+\Gamma} , \qquad \text{(IV.15)}$$

where $\gamma = \gamma^R + \gamma^{NR}$ allows for nonradiative decay apart from IVR. The relaxed yield is then

$$Y_{\text{rel}} = \frac{\gamma^R}{\gamma} - Y_{\text{dir}} = \frac{\gamma^R \Gamma}{\gamma(\gamma+\Gamma)} - \frac{\gamma^R}{N\gamma} . \qquad \text{(IV.16)}$$

Both Y_{dir} and Y_{rel} approach the correct statistical limits as $N \to \infty$. While the trends established by Eq. (IV.15) and (IV.16) are not applicable to the shortest alkyl chains with low vibrational excitation because N is too small for the egalitarian mixing model to be valid, these results are satisfactory for the higher density of states domain where they are in accord with experiments.

Even if shorter pulse experiments cannot be performed, it is possible to directly test (IV.14) by the following experiment: Para alkyl disubstitution should leave the absorption spectrum to modes 6b and 18a unshifted because this vibration has nodes in para positions (etc., for 12 and meta substitution). The density of states is similar (but less) in, say, the diethyl substituted benzene than in butyl benzene, but the coupling W_{sl_0} is roughly doubled because it is channeled through two bonds. Hence, the disubstitution at constant density of states should increase the relaxed yield with respect to the unrelaxed one. Of course, the short decay rate is quickened by this disubstitution of constant density of states.

V. QUANTUM BEATS

In the previous section we assumed that quantum beats in the fluorescence spectrum are not observed. This is always the situation in bulk room temperature experiments involving relatively large molecules. The initial thermal distribution of rotational states is carried over into the excited state, and any oscillations in the fluorescence originated in these incoherently excited rotational levels are averaged out. Even in the super-
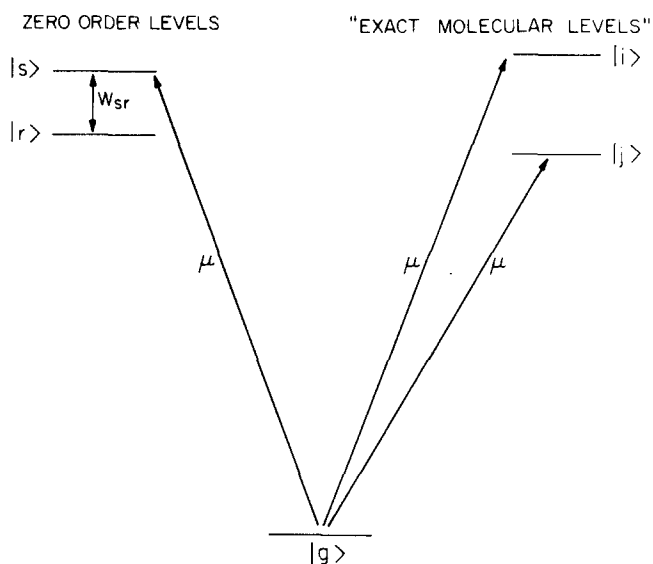
ZERO ORDER LEVELS   "EXACT MOLECULAR LEVELS"

FIG. 5. A three level model for quantum beats.

sonic jet experiments of Smalley et al.,[16] the large moments of inertia of the alkylated benzenes imply that with the beam temperature of ~2 °K the absorption lines are composed of several unresolved rotational components. Quantum beats are therefore not expected and are not observed in these experiments. With smaller molecules and lower beam temperature the rotational structure can be eliminated and beats can be observed as was recently demonstrated by McDonald and co-workers.[35]

The observability of quantum beats in the molecular fluorescence depend on one additional factor related to the theorem stated in Sec. IV and proven in Appendix A. To understand the implication of this theorem consider the three level model displayed in Fig. 5. The ground level $|g\rangle$ is radiatively coupled to zero order level $|s\rangle$ but not to $|r\rangle$, $|s\rangle$ and $|r\rangle$ are coupled by the intramolecular coupling W. Partial diagonalization of the Hamiltonian leads to the exact molecular levels $|i\rangle$ and $|j\rangle$ which are linear combinations of the wave functions $|s\rangle$ and $|r\rangle$ which diagonalize the Hamiltonian $H_0^M + W$. Both $|i\rangle$ and $|j\rangle$ contain contributions from $|s\rangle$ and both are therefore coupled radiatively to $|g\rangle$. We assume that the energy spacing $E_{ij} = E_i - E_j$ is large relative to the level widths so that levels $|i\rangle$ and $|j\rangle$ can be selectively excited. A broad band short time pulse excitation of the system which is initially in state $|g\rangle$ leads to a coherent linear combination of the $|i\rangle$ and $|j\rangle$ states

$$\Psi(t=0) = |s\rangle = a_{si}|i\rangle + a_{sj}|j\rangle , \qquad (V.1)$$

which evolve in time according to

$$\Psi(t) = a_{si}\exp(-iE_i t - \tfrac{1}{2}\gamma_i t)|i\rangle + a_{sj}\exp(-iE_j t - \tfrac{1}{2}\gamma_j t)|j\rangle , \qquad (V.2)$$

where γ_i and γ_j the (radiative) widths of levels $|i\rangle$ and $|j\rangle$. For times longer than the inverse energy spacing E_{ij}^{-1} the emission spectrum can be resolved; the intensity of the line of energy E_{jg} is $\gamma_j P_j(t) = \gamma_j|a_{sj}|^2 \exp(-\gamma_j t)$. As long as these two emission components are resolved, no quantum beats are expected in the corresponding intensities.

Consider now the total integrated intensity. We have shown in Appendix A that this is proportional to the population of the zero order $|s\rangle$ level, given by

$$P_s(t) = |\langle s | \Psi(t)\rangle|^2$$
$$= |a_{si}|^4 \exp(-\gamma_i t) + |a_{sj}|^4 \exp(-\gamma_j t)$$
$$+ 2|a_{si}|^2|a_{sj}|^2 \exp[-\tfrac{1}{2}(\gamma_i + \gamma_j)t]\cos(E_{ij}t) .$$
$$(V.3)$$

Quantum beats should be observed in the integrated intensity for $E_{ij} > \tfrac{1}{2}(\gamma_i + \gamma_j)$. We conclude that the observability of quantum beats in fluorescence spectra depends on the mode of detection: beats are not expected in the resolved components but, when other conditions are satisfied, should be observed in the total intensity of the emission which correspond to a particular zero order level.

This conclusion is in accord with recent experiments of Lauberau and co-workers,[36] where quantum beats were observed due to the coherent excitation of the vibrational states of different isotopes of liquid CCl_4. The beats are observed in the total coherent anti-Stokes scattering intensity, but can be suppressed by employing a spectral resolution sufficient to separate the anti-Stokes scattering from the different isotopes. In the quantum beat experiments of McDonnald and co-workers[35] beats are observed between levels whose spacing exceeds their widths so finer resolution of the emission can suppress some of the beating behavior.

VI. CONCLUSION

Intramolecular vibrational relaxation (IVR) has been a vaguely defined process. The rate of energy transfer between modes depends on the representation and on the modes chosen, and it is not clear that such a rate, obtained for example from classical trajectory simulations, is directly related to any observable quantity. A more direct approach considers the observable properties such as linewidths of absorption or excitation spectra (e.g., overtone line shapes in large molecules[7,8]) or the time evolution of molecular fluorescence. In this paper we have considered the later phenomenon which was observed in recent experimental studies.[16,17] Emphasis here is placed upon a consideration of the observable energy and/or time resolved characteristics of the emission spectrum for a variety of experimentally feasible initial states of the system. The intramolecular vibrational relaxation rates are associated with the time scales over which this emission spectrum changes from that of the initially prepared state to that assoicated with the relaxed states. The use of a realistically measurable time scale is necessary in order to eliminate wide variations in estimated IVR relaxation rates which arise from the choice of (a) an unpreparable initial state of the system, (b) a nonmeasurable IVR time scale, (c) a static (i.e., based on quantum yield measurements) definition of IVR rates, (d) a crude zeroth order representation of the system, or (e) combinations of these.

The theory builds heavily on known results from the theory of electronic relaxation processes, and this leads us to consider the intermediate and statistical limits of

intramolecular vibrational relaxation processes.[15(a)] In the intermediate case the density of vibrational levels is not high enough to drive truely irreversible IVR; however, on short enough and potentially observable time scales, the system can appear to undergo IVR. This arises when the system is initially prepared in a nonstationary state which is a linear superposition of a number of vibrational eigenstates. At the initial time these vibrational eigenstates have definite phase relationships with each other. As time evolves, the initial phase coherence between the vibrational eigenstates is destroyed because of the differing energies of the eigenstates. This is an "intramolecular dephasing" process which is equivalent on this short time scale to the IVR observed in the statistical limit. In the latter case the vibrational density of states is high enough to make this process irreversible.

In the intermediate case the IVR does not contribute to *individually* resolved level line broadening, while the statistical limit has IVR induced broadening.

In order to explicitly consider the effects of IVR on the molecular emission spectrum, it is necessary to generalize the electronic relaxation theory to incorporate the radiative decay characteristics of the dense vibrational manifold along with the nature of the emission spectra associated with these states. We have carried this generalization and used it to analyze the experiments of Smalley and co-workers[16] on the structure and the dynamics of the emission from alkylated benzenes. The following observations were used in this analysis: (a) As mentioned above, during the initial dephasing an intermediate state molecule behaves as a statistical limit molecule[33] (b) The fact that the benzene ring–alkyl chain coupling is transmitted through the bond connecting them implies that this dephasing time is independent of the alkyl chain length. (c) The fluorescence spectrum evolves in time only during this dephasing. These observations immediately imply that the time scale for evolution of the fluorescence structure will be approximately the same for all the alkyl benzenes studied experimentally. This time is expected to be of the order 10^{-11}–10^{-12} sec as observed in the experiment of Parmenter and co-workers.[17] It could not be observed in the nanosecond time scale experiments of Smalley's group.

In contrast to the predicted lack of variation in the time evolution our theory predicts considerable changes in the relative yields of the relaxed and unrelaxed emission spectra as the alkyl chain of the alkyl benzene molecules become longer, i.e., as the molecule changes from the intermediate to the statistical limit.

If the experiments are coherently exciting the zeroth order vibrational state $|s\rangle$, this prediction is in accord with the experimental observations. Alternatively, the excitation pulse duration may be too long, so only a few of the vibrational eigenstates $|j\rangle$ are excited by the laser. Then shorter excitation pulses are required to coherently excite the full $|s\rangle$. The use of dialkyl substituted benzenes may be a useful method for varying the effective intramolecular coupling strength to test

these considerations further.

In the sparse intermediate case quantum beats in the emission intensity may also occur. We have seen that the observability of beats depends on the mode of detection. In particular, when the emission spectrum can be resolved to components associated with individual excited levels, beats are observable only in the frequency integrated intensity.

The theoretical analysis discusses in detail the time variation of the relaxed and unrelaxed emission spectra and yields for both short pulse and long time experiments utilizing an egalitarian mixing model for the intermediate case which approaches the proper statistical limit behavior. For theoretical analysis of intermediate duration pulses and for more detailed resolution of the spectrum it is probably desirable to consider direct computer simulations of typical models.[33]

ACKNOWLEDGMENTS

APPENDIX A

Here we prove the following theorem: Consider the model displayed in Fig. 4. After an initial excitation preparing the system in (zero order) level $|s\rangle$, the integrated emission intensity associated with transition into ground level $|m_r\rangle$, which is coupled exclusively to zero order excited level $|r\rangle$, is proportional at all times t to the population $P_r(t) = |\langle r | \exp(-iHt) | s\rangle|^2$ of the level $|r\rangle$.

Denote by $|m_r k\rangle$ the molecular level $|m_r\rangle$ dressed by the photon state $|k\rangle$ ($|m_r k\rangle = |m_r\rangle |k\rangle$). $|m_r k\rangle$ is an eigenstate of the zero order Hamiltonian $H_0 = H_0^M + H_0^R$. In what follows the subscript r on m_r is disregarded. We want to calculate the time dependent frequency integrated intensity $I_m(t)$ defined by

$$I_m(t) = \frac{d}{dt} \sum_k P_{mk}(t) , \tag{A1}$$

where

$$P_{mk}(t) = |\langle mk | \exp(-iHt) | s\rangle|^2 . \tag{A2}$$

$P_{mk}(t)$ may also be written in the form

$$P_{mk}(t) = \frac{|\langle m | \mu | r\rangle|^2}{4\pi^2}$$

$$\times \lim_{\eta \to 0^+} \left(\left| \int_{-\infty}^{\infty} dE \exp(-iEt) \frac{1}{E - E_{mk} + i\eta} G_{rs}(E + i\eta) \right|^2 \right) , \tag{A3}$$

where $G(E + i\eta) = (E + i\eta - H)^{-1}$. Using the convolution theorem we can write the term inside the absolute value signs as

$$\int_{-\infty}^{\infty} dE \exp(-iEt) \mathcal{A}_{mk}(E) ,$$

where

$$\mathcal{A}_{mk}(E) = \int_{-\infty}^{\infty} dU \; \frac{1}{U - E_{mk} + i\eta} \; \frac{1}{U - E - E_{mk} - i\eta}$$

$$\times \left(\frac{1}{U - H + i\eta}\right)_{rs} \left(\frac{1}{U - E - H - i\eta}\right)_{rs} . \quad \text{(A4)}$$

We now perform the summation over the photon states k by converting it to an integration. The limits of this integration can be taken to a good approximation to be $\pm\infty$. This gives

$$\sum_k \frac{1}{(U - E_{mk} + i\eta)(U - E - E_{mk} - i\eta)} \simeq \frac{2\pi i \rho_{mk}}{E + 2i\eta} , \quad \text{(A5)}$$

where ρ_{mk} is the density of photon states dressing the molecular level m. Denote

$$2\pi |\mu_{m,r}|^2 \rho_{mk} = \gamma_{m\to r}^R . \quad \text{(A6)}$$

$\gamma_{m\to r}^R$ is the contribution to the radiative width of the level r due to its decay into level m. We obtain

$$P_m(t) \equiv \sum_k P_{mk}(t) = \frac{i\gamma_{m\to r}^R}{4\pi^2} \int_{-\infty}^{\infty} dE \; \frac{\exp(-iEt)}{E + 2i\eta}$$

$$\times \lim_{\eta\to 0^+} \left[\int_{-\infty}^{\infty} dU \left(\frac{1}{U - H + i\eta}\right)_{rs} \left(\frac{1}{U - E - H - i\eta}\right)_{rs}\right] . \quad \text{(A7)}$$

From Eq. (A7) it follows that

$$I_m(t) = \frac{d}{dt} P_m(t) = \gamma_{m\to r}^R P_r(t) , \quad \text{(A8)}$$

where the last equality arises because

$$P_r(t) = |\langle r | \exp(-iHt) | s \rangle|^2$$

$$= \lim_{\eta\to 0^+} \left[\frac{1}{4\pi^2} \int dE \exp(iEt) \int_{-\infty}^{\infty} dU \left(\frac{1}{U - Hi\eta}\right)_{rs}\right.$$

$$\left. \times \left(\frac{1}{U - E - H - i\eta}\right)_{rs}\right] . \quad \text{(A9)}$$

The second equality in Eq. (A9) is verified by the same procedure which leads to Eqs. (A3) and (A4).

APPENDIX B

Here we briefly outline the solution to the random coupling model of IVR defined as follows: a dense (level spacing small compared to level width or to the inverse experimental timescale) set of levels $\{|l\rangle\}$ constitute a solution to a given zero order approximation (eigenstates of H_0). A residual perturbation W couples these levels to each other. The matrix elements $W_{ll'}$ are random functions of the state indices l and l'. Given that at $t = 0$ only one particular level $|s\rangle$ is populated, we want to know the population of this level as well as some other level $|r\rangle$ at time t. We use the diagramatic approach advanced by Carmeli and Nitzan[32] for random intercontinuum coupling models. The coupling $W_{ll'}$ is assumed to be a real Gaussian random function of the indices l, l' with

$$\langle W_{ll'} \rangle = 0 , \quad \text{(B1)}$$

$$\langle W_{ij} W_{kl} \rangle = \langle W_{ij}^2 \rangle (\delta_{ik}\delta_{jl} + \delta_{il}\delta_{jk}) . \quad \text{(B2)}$$

The averages are defined as in Ref. 32. We have to evaluate

$$P_b(t) = \frac{1}{2\pi i} \int_{-\infty}^{\infty} dE \exp(-iEt) \langle G_{bb,ss}(E) \rangle , \quad \text{(B3)}$$

where $G_{bb,ss}$ ($b = s$ or r) is a matrix element of the tetradic Green's function

$$G_{bb,ss} = \frac{1}{2\pi i} \int_{-\infty}^{\infty} dU \left(\frac{1}{U - H + i\eta}\right)_{bs} \left[\frac{1}{U - E - H - i(\eta' - \eta)}\right]_{sb}$$

$$(\eta, \eta' \to 0; \; \eta' > \eta) , \quad \text{(B4)}$$

where $H = H_0 + W$ and where all the state indices refer to eigenfunctions of H_0:

$$H_0 | b \rangle = (E_b + i\gamma) | b \rangle . \quad \text{(B5)}$$

We first calculate

$$B_{bs} \equiv \langle (U - H + i\eta)_{bs}^{-1} [U - E - H - i(\eta' - \eta)]_{sb}^{-1} \rangle \quad \text{(B6)}$$

by expanding in powers of W and doing the averaging by pairing the interaction terms. As all states belong to the same manifold, there is only one kind of propagator and one kind of vertex. The propagators associated with levels $|s\rangle$ and $|r\rangle$ are specially marked by the corresponding letters. The following examples should clarify the diagramatic notation:

$$\bullet = V_{ll'} ,$$

$$\underline{\quad b \quad} = \begin{cases} (U - E_b + \tfrac{1}{2} i\gamma)^{-1} & \text{(upper branch)} , \\ (U - E - E_b - \tfrac{1}{2}i\gamma)^{-1} & \text{(lower branch)} , \end{cases}$$

$$s \overset{\frown}{\bullet\quad\bullet} s = (U - E_s + \tfrac{1}{2} i\gamma)^{-2} \sum_l \frac{\langle W_{sl}^2 \rangle}{U - E_l + \tfrac{1}{2} i\gamma}$$

$$\text{(upper branch)} ,$$

$$\begin{array}{c} s \overset{\frown}{\bullet\quad\bullet} r \\ s \;\bullet\quad\bullet\; r \end{array} = [(U - E_s + \tfrac{1}{2} i\gamma)(U - E - E_s - \tfrac{1}{2} i\gamma)$$

$$\times (U - E_r + \tfrac{1}{2} i\gamma)(U - E - E_r - \tfrac{1}{2} i\gamma)]^{-1}$$

$$\times \sum_l \frac{\langle W_{sl}^2 \rangle \langle W_{rl}^2 \rangle}{(U - E_l + \tfrac{1}{2} i\gamma)(U - E - E_l - \tfrac{1}{2} i\gamma)} .$$

The present situation is slightly different from that considered by Carmeli and Nitzan,[32] where coupling exists only between states which belong to different manifolds and therefore only one product of δ functions contributes in Eq. (B2). However, the survival rules for different diagrams remain essentially the same. Defining the dressed propagator

$$\Longleftrightarrow = \underline{\quad\quad} + \underline{\overset{\frown}{\bullet\quad\bullet}} +$$

$$+ \underline{\overset{\frown}{\bullet\quad\bullet}\;\overset{\frown}{\bullet\quad\bullet}} + \cdots$$

$$= \begin{cases} (U - \tilde{E}_b + \tfrac{1}{2} i\tilde{\Gamma})^{-1} & \text{(upper branch)} , \\ (U - E - \tilde{E}_b - \tfrac{1}{2} i\tilde{\Gamma})^{-1} & \text{(lower branch)} , \end{cases} \quad \text{(B7)}$$

where

$$\tilde{\Gamma} = \gamma + \Gamma = \gamma - 2 \operatorname{Im}\left(\lim_{\eta\to 0} \sum_l \frac{\langle W_{bl}^2 \rangle}{E - E_l + \tfrac{1}{2} i\gamma}\right)$$

$$= \gamma + 2\pi \overline{W_{bl}^2} \rho_l \quad \text{(B8)}$$

and

$$\tilde{E}_b = E_b + PP \sum_l \frac{\langle W_{bl}^2 \rangle}{E - E_l} \quad .$$ (B9)

The leading contribution to B_{ss} is found to be

$$B_{ss} = \left\langle \overbrace{\underline{}}^{s} \right\rangle = [(U - \tilde{E}_s + \tfrac{1}{2} i \tilde{\Gamma})(U - E - \tilde{E}_s - \tfrac{1}{2} i \tilde{\Gamma})]^{-1} ,$$ (B10)

which, using Eqs. (B3) and (B4), lead to

$$P_s(t) = \exp(-\tilde{\Gamma} t) \quad .$$ (B11)

The leading contribution to B_{rs} is identified as

(B12)

(B13)

Direct calculation yields

$$\square = \frac{\langle W^2 \rangle \,(E + i\tilde{\Gamma})}{E + i\gamma} \quad ,$$ (B14)

whence

$$B_{rs} = \frac{\langle W^2 \rangle \,(E + i\tilde{\Gamma})}{E + i\gamma} \; \frac{1}{\left(U - \tilde{E}_s + \dfrac{i}{2}\tilde{\Gamma}\right)\left(U - E - \tilde{E}_s - \dfrac{i}{2}\tilde{\Gamma}\right)\left(U - \tilde{E}_r + \dfrac{i}{2}\tilde{\Gamma}\right)\left(U - E - \tilde{E}_r - \dfrac{i}{2}\tilde{\Gamma}\right)} \quad .$$ (B15)

Equation (B15) together with Eqs. (B4) and (B3) lead after a straightforward calculation to the result (IV.12b).

[1](a) H. Schröder, H. J. Neusser, and E. W. Schlag, Chem. Phys. Lett. 54, 4 (1978); (b) J. C. Hsieh, C. S. Huang, and E. C. Lim, J. Chem. Phys. 60, 4345 (1974).

[2](a) R. K. Sander, B. Soep, and R. N. Zare, J. Chem. Phys. 64, 1242 (1976); (b) R. Naaman, D. M. Lubman, and R. N. Zare, J. Chem. Phys. 71, 4192 (1979).

[3]S. Okajima and E. C. Lim, Chem. Phys. Lett. 37, 403(1976).

[4]H. S. Kwok and E. Yablonovitch, Phys. Rev. Lett. 41, 745 (1978).

[5]T. F. Deutch and S. J. Brueck, Chem. Phys. Lett. 54, 258 (1978); D. S. Frankel, J. Chem. Phys. 65, 1696 (1976).

[6](a) B. Kopainsky and W. Kaiser, Chem. Phys. Lett. 66, 39 (1979); (b) J. P. Maier, A. Seilmeir, A. Laubereau, and W. Kaiser, Chem. Phys. Lett. 46, 527 (1977).

[7]R. G. Bray and M. J. Berry, J. Chem. Phys. 71, 4909 (1979).

[8]J. W. Perry and A. H. Zewail, J. Chem. Phys. 70, 582 (1979); Chem. Phys. Lett. 65, 31 (1980).

[9]I. Oref and B. S. Rabinovitch, Acc. Chem. Res. 12, 166 (1979) and references therein.

[10]P. J. Nagy and W. L. Hase, Chem. Phys. Lett. 54, 73 (1978).

[11]B. Soep, C. Michel, A. Tramer, and L. Lindquist, Chem. Phys. 2, 293 (1973).

[12]K. F. Freed, Faraday Discuss. Chem. Soc. 67, 231 (1979).

[13]See, for example, C. K. N. Patel, A. C. Tam, and R. J. Kerl, J. Chem. Phys. 71, 1470 (1979); B. R. Henry, Acc. Chem. Res. 10, 207 (1977); R. Wallace, J. Chem. Phys. 11, 189 (1975); M. E. Long, R. L. Swofford, and A. C. Albrecht, Science 191, 183 (1976); M. S. Burberry and A. C. Albrecht,

J. Chem. Phys. 70, 147 (1979).

[14]D. D. Smith and A. H. Zewail, J. Chem. Phys. 71, 540 (1979).

[15](a) K. F. Freed, Chem. Phys. Lett. 42, 600 (1976); (b) A. Nitzan and J. Jortner, J. Chem. Phys. 71, 3524 (1979).

[16](a) J. B. Hopkins, D. E. Powers, and R. E. Smalley, J. Chem. Phys. 71, 3886 (1979); 72, 2905(E) (1980); (b) J. B. Hopkins, D. E. Powers, S. Mukamel, and R. E. Smalley, J. Chem. Phys. 72, 5049 (1980); (c) J. B. Hopkins, D. E. Powers, and R. E. Smalley, J. Chem. Phys. 73, 683 (1980).

[17]R. A. Coveleskie, D. A. Dolson, and C. S. Parmenter, J. Chem. Phys. 72, 5774 (1980).

[18]S. Mukamel and R. E. Smalley (unpublished).

[19]References to the intermediate case can be found in later works by Smalley et al. [14(d)]

[20](a) A. Nitzan, J. Jortner, and R. Rentzepis, Proc. R. Soc. (London) Ser. A 37, 367 (1972); (b) A. Frad, F. Lahmani, A. Tramer, and C. Tric, J. Chem. Phys. 60, 4419 (1974); (c) R. van der Werf and J. Kommandeur, Chem. Phys. 16, 125 (1976).

[21]For reviews of theories of electronic radiationless relaxation see, for example, (a) K. F. Freed, Topics Appl. Phys. 15, 23 (1976); Acc. Chem. Res. 11, 74 (1977); Adv. Chem. Phys. 42, 207 (1980); (b) S. Mukamel and J. Jortner, in Excited States, edited by E. C. Lim (Academic, New York, 1977), Vol. III.

[22]The inequality $n_a' < n_a$ is used as a shorthand expression for $\sum_\alpha n_{ea}^{\alpha'} \omega_{e\alpha} < \sum_\alpha n_{ea}^{\alpha} \omega_{e\alpha'}$.

[23]The nonradiative damping matrix γ^{NR} may be assumed to be diagonal both in the zero order and the exact representations because of the expected random nature of the nonradiative

electronic coupling. (B. Carmeli and A. Nitzan, unpublished results.)

[24] S. Mukamel and A. Nitzan, J. Chem. Phys. 66, 2462 (1977).

[25] A. Nitzan, J. Jortner, and P. Rentzepis, Mol. Phys. 22, 585 (1971).

[26] A. Nitzan, Chem. Phys. 41, 163 (1979).

[27] If the molecule is initially in state $|m_s\rangle$ a broad band pulse will prepare it in state $|s\rangle$. If it is initially is state $|m_r\rangle$ similar excitation will prepare it in state r.

[28] See, for example, Ref. 20(a).

[29] K. F. Freed, J. Chem. Phys. 52, 1345 (1970).

[30] M. L. Goldberger and R. M. Watson, Collision Theory (Wiley, New York, 1969).

[31] W. M. Gelbart, S. A. Rice, and K. F. Freed, J. Chem. Phys. 61, 936 (1974); S. D. Druger, J. Chem. Phys. 67, 3238, 3249 (1977).

[32] B. Carmeli and A. Nitzan, J. Chem. Phys. 72, 2054 (1980); 72, 2070 (1980).

[33] B. Carmeli, I. Scheck, A. Nitzan, and J. Jortner, J. Chem. Phys. 71, 1928 (1980); W. M. Gelbart, D. F. Heller, and M. L. Elert, Chem. Phys. 7, 116 (1975).

[34] S. M. Beck and S. Mukamel (unpublished).

[35] J. Chaiken, T. Benson, M. Gurnick, and J. D. McDonald, Chem. Phys. Lett. 61, 195 (1979).

[36] A. Lauberau, G. Wochner, and W. Kaiser, Opt. Commun. 17, 91 (1976).